

Evolution of the Malignant Bone Marrow with Successful Therapy – Quantitative Analysis with Whole-body Diffusion-weighted MRI

Danoob Dalili¹; Priya V. Joshi²; Robert Grimm³; Anwar R. Padhani⁴

¹ Imperial College Healthcare NHS Trust, St Mary's Hospital, London, United Kingdom

² Mount Vernon Cancer Centre and the East and North Herts NHS trust hospitals, Northwood, Middlesex, United Kingdom

³ Siemens Healthineers, Erlangen, Germany

⁴ Paul Strickland Scanner Centre, Mount Vernon Cancer Centre, Northwood, Middlesex, United Kingdom

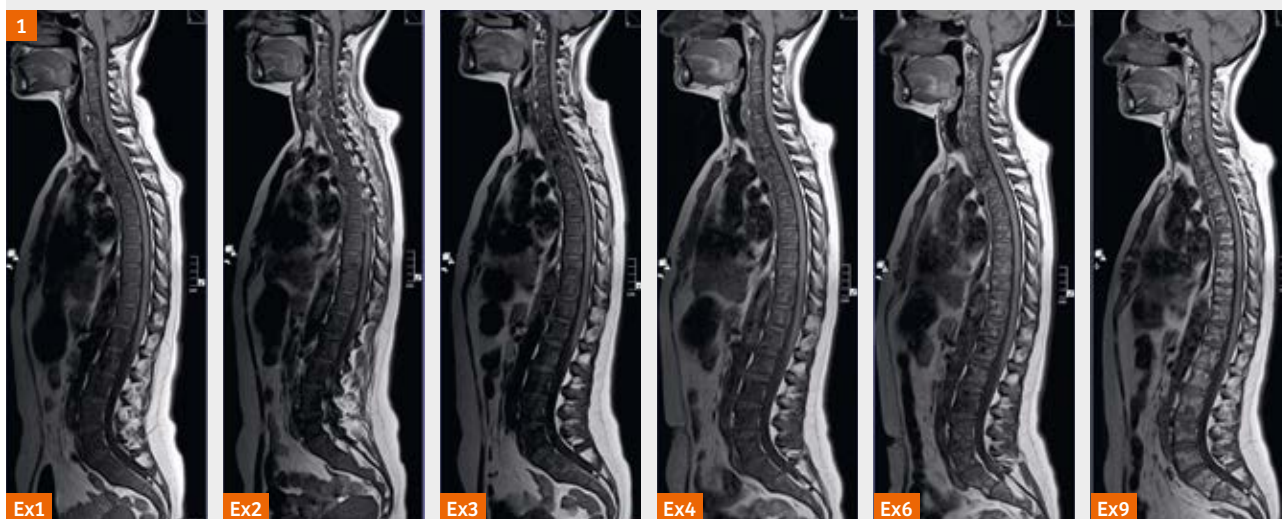
Introduction

Bone disease is a common occurrence in metastatic breast cancer (MBC), but accurate evaluation of treatment benefit is notoriously difficult to do. There is a critical clinical need to develop non-invasive biomarkers to assess therapeutic effects of bone involvement in MBC. This is because the detection of primary non-responders and secondary therapy failure when disease burden is lowest, can help guide therapy decisions [1]. Currently, imaging assessments can only determine bone disease progression, because of which many patients with bone predominant disease receive ineffective medications for prolonged periods, and as a result do not change treatments until disease burdens become large, thus potentially hindering

the effectiveness of follow-on treatments. It has been suggested, that aggressive disease detection methods and response monitoring could promote precision oncology in patients with bone involvement in MBC [2].

Guidelines from the American Society of Clinical Oncology and the European School of Oncology have recognized these limitations, advocating the use of serum tumor markers in addition to clinical assessments and imaging for monitoring MBC response [3, 4]. There is however, confusion regarding what constitutes suitable imaging for bone disease monitoring. All guidelines advocate the use of computed tomography (CT) and bone scans (BS), thus side stepping the limitations of CT/BS for assessing response in women with bone predominant metastatic disease.

Figure 1: Serial changes on morphological whole-spine sagittal T1-weighted images.



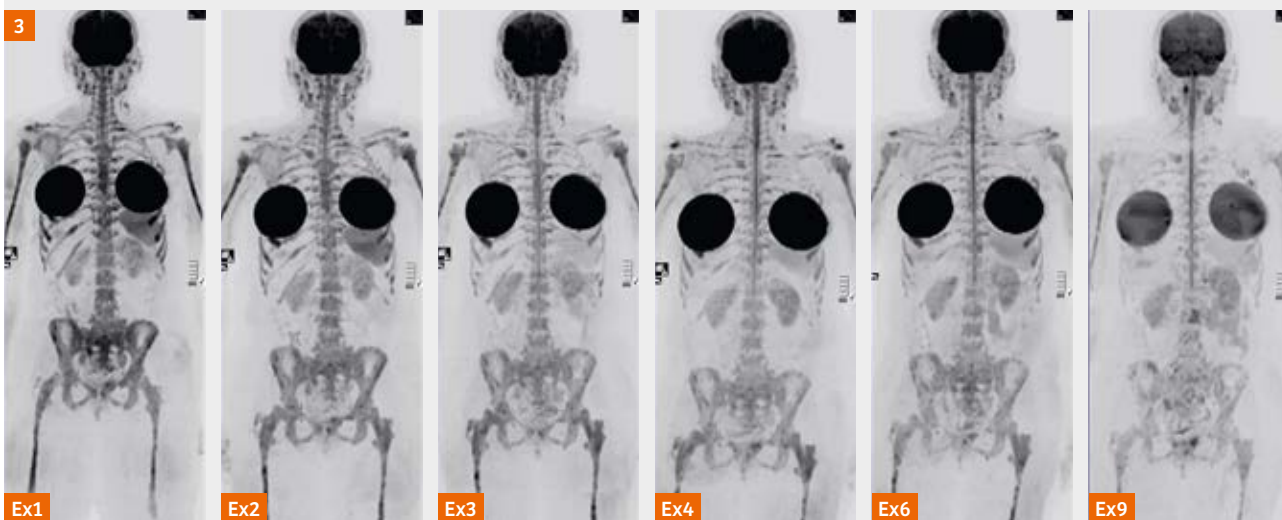
Diffuse metastatic infiltration throughout the spine, however note the small amount of fat on examination 6 (Ex6). The re-emergence of fat signal intensity is best appreciated on the last study (Ex9). The nature of the darker background signals on Ex9 is uncertain, but bone marrow (BM) scarring and/or residual active disease must be considered.

Figure 2: Serial changes on sagittal whole-spine STIR images.



Diffuse metastatic infiltration throughout the spine. Note no appreciable change in signal intensity between Ex1 and Ex2. There is a marked increased in bone marrow signal between Ex3 and Ex6 consistent with increased BM water, which fades on the last examination (Ex9).

Figure 3: Serial changes on whole-body b = 900 s/mm² 3D MIP images (inverted scale).



b900 3D MIP images (inverted scale) demonstrate a gradual reduction in signal intensity throughout the course of treatment, which is most evident between Ex1 and Ex2. The signal intensity is lowest on the last examination (Ex9). No extra-osseous disease is detected. Bilateral breast implants are seen in situ.

There is accumulating evidence showing the added value of PET/CT and whole-body MR imaging (WB-MRI) for decision making in metastatic breast cancer [5, 6]. WB-MRI with morphological and diffusion-weighted sequences has emerged as powerful tool for detecting and assessing the response of MBC with good efficacy in the assessment of bone metastases [7]. The key advantage of WB-MRI is

that the success of therapies can be positively assessed (CT/BS scans use the ‘no evidence of progression’ category as meaning therapy success). As a result, WB-MRI has the potential to alter clinical diagnostic thinking when assessing bone disease response [6]. Uniquely, quantitative apparent diffusion coefficient values (ADC; unit $\mu\text{m}^2/\text{s}$) can bring objectivity to therapy response assessments.

Figure 4: Serial changes on MIP-ADC projection images.



Top row: ADC color projections focusing on response showing serial changes in voxels that are highly likely to be responding (green). Marked response is first observed on Ex3 in voxels co-localized to the axial skeleton. These high ADC voxels only decrease in extent on Ex9.

Bottom row: ADC color projections focusing on marrow showing serial changes in voxels that are likely to represent normal bone marrow (yellow). Their appearance is co-localized to the appendicular skeleton (proximal humeri and femora). The appearance of fat in the spine on Ex9 shown on T1w images in Figure 1 cannot be readily appreciated on these projection images.

Semi-automated threshold-based, quantitative ADC mapping and histogram analysis has been introduced as a viable and efficient tool for whole-body ADC mapping [8].

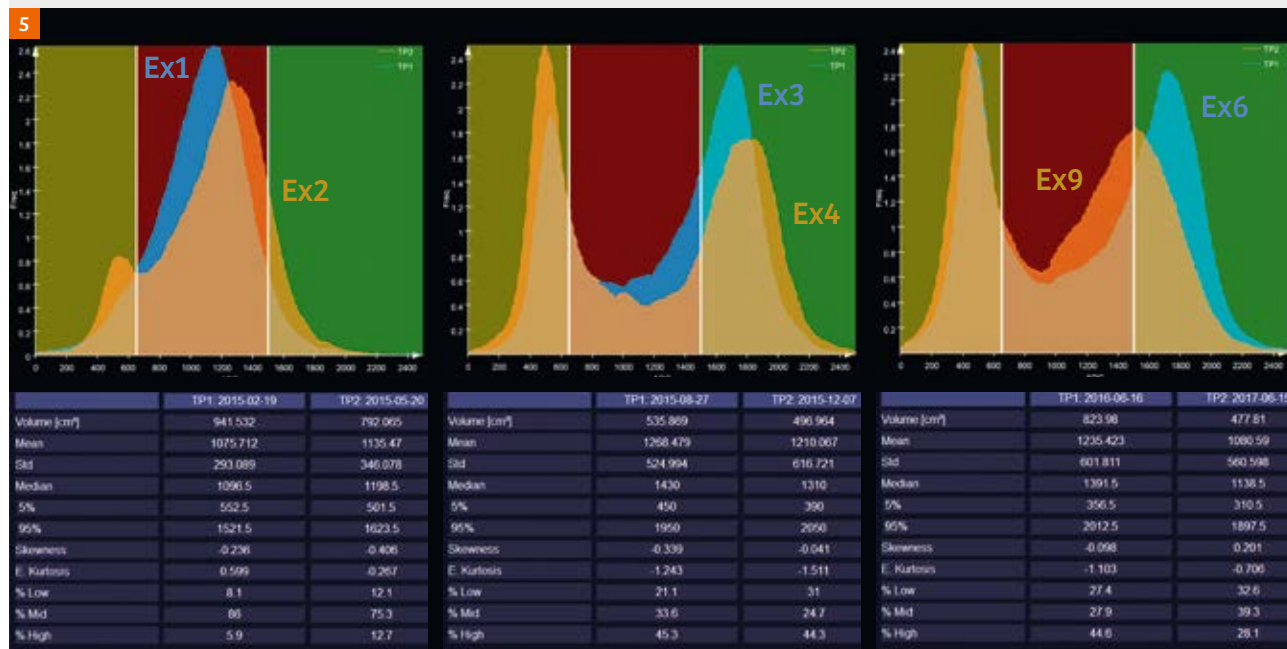
This case report applies the methodology of the companion article by Dalili et al. on the ability of the *syngo.via* Frontier MR Total Tumor Load software¹ to distinguish ADC changes ascribable to tumor response and bone marrow recovery [9]. We discuss how ADC changes can be explained by the mechanism of tumor cell death and introduce a biologic model that explains imaging observations during the repair phase after effective therapy [10].

¹ *syngo.via* Frontier is for research only, not a medical device.
syngo.via Frontier MR Total Tumor Load is a released research prototype.

Case study

A 49-year-old peri-menopausal woman presented with bone only metastatic lobular carcinoma (ER-positive, HER2-neu negative) in 2013. Bilateral mastectomy (left breast for risk reduction), axillary node clearance and breast reconstructions were performed with completion radiotherapy to the right supraclavicular fossa and chest wall. She underwent initial systemic anticancer therapy with Tamoxifen and Zoledronic acid infusions. During treatment, she developed bone pain but CT scans were unhelpful regarding the status of her bone disease. Subsequently she was referred for a whole-body MRI scan to assess her disease status (volume and tumor viability). Nine WB-MRI studies were then performed every 3–4 months over the next 3.5 years for therapy response assessments.

Figure 5: ADC histogram changes with time.



Histograms were created using the methodology of the accompanying article [9] at each time point. Fixed ADC thresholds were chosen (650 and 1500 $\mu\text{m}^2/\text{s}$) because examination 1 was an 'on treatment' (Tamoxifen and Zoledronic acid) study (that is, no true pre-therapy baseline study was available). These default thresholds are based on literature values [12, 13]. Therefore, voxels in the red range are likely to represent untreated disease or those that have no-detected response. Green colored voxels have ADC values $\geq 1500 \mu\text{m}^2/\text{s}$ (representing voxels that are 'likely' to be responding). Yellow voxels lie below $650 \mu\text{m}^2/\text{s}$ and represent regions 'likely' to represent normal bone marrow.

Ex1 Ex2: At baseline (Ex1), the histogram is negatively skewed (tail to the left) consistent with the therapy effects of Tamoxifen, although 86% of segmented voxels are in the active range (between $650\text{--}1500 \mu\text{m}^2/\text{s}$). With the change of treatment to Anastrozole and Goserelin (Ex2), a positive therapy change effect can be detected with a small right sided shift of the histogram. The bulk of the voxels on Ex2 (75%), remain in the red-voxel range ($650\text{--}1500 \mu\text{m}^2/\text{s}$). The emergence of a new peak below $650 \mu\text{m}^2/\text{s}$ is noteworthy and, these yellow voxels seem confined to the limb bones (Fig. 4 – bottom row).

Ex3 Ex4: With the change of treatment to Everolimus and Exemestane (Ex3), a more dramatic histogram change becomes visible with 2 well separated peaks (below $650 \mu\text{m}^2/\text{s}$ and above $1500 \mu\text{m}^2/\text{s}$). The peak above $1500 \mu\text{m}^2/\text{s}$ indicates large cell kill and highly likely response and these green voxels can be located to the axial skeleton (Fig. 4 – top row). The enlarging peak below $650 \mu\text{m}^2/\text{s}$ is consistent with further return of the mixed bone marrow depicted as yellow areas in the limb bones (Fig. 4 – lower row). This twin peak histogram pattern does not change much in the 6 month period between Ex4–Ex6.

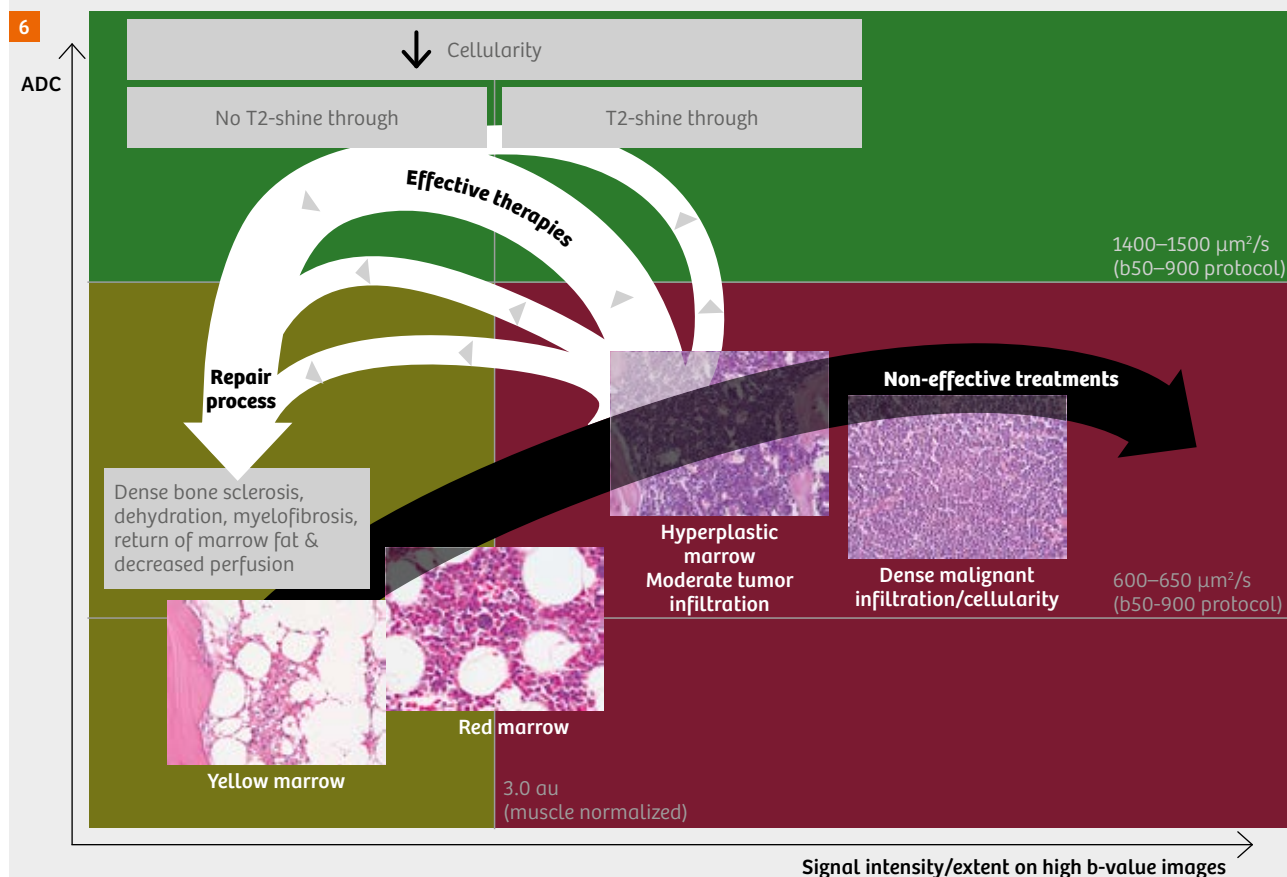
Ex6 Ex9: A change of the histogram becomes visible 12 months later, on Ex9. At this point, the higher peak of the ADC histogram has begun to shift towards the red region, visible as increasing red regions on the MIP-ADC low projection images in Fig. 4. However, these emerging red voxels are unlikely to represent tumor regrowth because the b900 signal intensity has remained low (Fig. 3) and fat has remerged in the marrow spaces (Fig. 1). So, it's most likely that the emerging red regions on Ex9 are likely to represent bone marrow scarring/bone sclerosis according to the model in Fig. 6. This remains to be confirmed.

After the first WB-MRI examination (examination 1), therapy was changed to Anastrozole and Goserelin with Zoledronic acid infusions. She remained symptomatic and a follow-up WB-MRI (examination 2) did not demonstrate appreciable cell kill to the therapy change. Subsequently she was switched to Exemestane and Everolimus (mTOR inhibitor) with good symptomatic relief of bone pain. Symptomatic relief of bone pain was accompanied by a good therapy effect on whole-body MRI scans (examinations 3 and 4). However, her blood hemoglobin levels remained below the normal range at 90 g/L between examinations 1 and 4. Eventually she returned to work and currently, she suffers only from minor drug

toxicity related side effects. Her hemoglobin recovered to the normal range by examination 6 (120 g/L) at 18 months, and improved further to 130 g/L by examination 9 at 30 months, thus confirming an overall good systemic response.

In this report, we illustrate six WB-MRI examinations, with the initial four studies performed consecutively at 3–4 month intervals (Ex1–Ex4) and the latter two (Ex6 and Ex9) at 18 months and 30 months respectively. All studies were undertaken using the same 1.5T MAGNETOM Avanto scanner, utilizing a published protocol [11]. The diffusion-

Figure 6: Biological model of the relationships between bone marrow state, high b-value signal intensity and ADC values in the setting of therapy response [10].



With therapy progression (black arrow), increases in the volume of abnormal signal intensity, new areas of abnormal signal intensity, or increased intensity of abnormalities on high b-value DW images can be seen. Modest increases, unchanged or slight decreases in ADC values compared to pre-therapy values can occur with disease progression. The initial modest increase in ADC values with disease progression occurs because tumor infiltration displaces bone marrow fat cells, increases bone marrow water (including water in the extracellular space) and increases tissue perfusion, thus returning higher ADC values compared to yellow or mixed bone marrow. The important point to note is that these increases in ADC values tend to be of small magnitude, provided that the metastatic lesions remain non-necrotic and in our experience rarely increases > 1400–1500 $\mu\text{m}^2/\text{s}$. Stable ADC values occur when unchanged tumor cellularity occurs with increases in the geographic extent of disease. Reductions in ADC values are probably related to increasing cellularity within a fixed bone marrow space.

A variety of high b-value signal and ADC changes can be seen with effective therapy (white arrows). Decreases in signal intensity on high b-value images accompanied by increases in ADC values is the usual pattern (thick white arrow). The extent of ADC increases seems to depend on the type of treatment given with higher ADC values for treatments that cause greater tumor cell death especially when there is a strong inflammatory component. Occasionally, unchanged or minimally decreased high signal intensity on high b-value images associated with marked rises in ADC values is observed, as in this case (Ex2–Ex6). This is termed ‘T2-shine through’ which also indicates a successful response to therapy. T2-shine through appearances often can take a long time (often more than 1 year) for b-value signal intensity and ADC to decrease to the normal levels. The emergence of bone marrow sclerosis, fibrosis and/or return of bone marrow fat are part of repair processes. Note that these repair processes can decrease b-value signal intensity without affecting ADC values.

weighted images of examinations were analysed using threshold-based segmentation with *syngo.via* Frontier MR Total Tumor Load prototype software¹ [8]. Response to treatment was displayed using the methodology described in the accompanying article [9].

Discussion

The premise for the use of ADC as a parameter of tissue characterization in the setting of treatment response, is that therapy-induced cell death precedes macroscopic lesion size changes. As a result of cellular necrosis, which results in loss of cell membrane integrity and increases in extracellular space water, ADC values typically increase.

¹ *syngo.via* Frontier is for research only, not a medical device.
syngo.via Frontier MR Total Tumor Load is a released research prototype.

During the following weeks to months, tumors may show shrinkage, with a resorption of the free extracellular fluid and fibrotic conversion leading to decreases in ADC values, although tumor recurrence can also result in reduced ADC values.

The degree of increase in ADC with successful therapy is highly dependent on the mode of cellular death with necrotic cell death resulting in higher ADC values due to associated inflammation and increased tissue water. Thus, chemotherapy typically results in greater degrees of tumor cell death and greater increases in ADC values [10]. With hormonal therapy, the mode of cell death is typically apoptotic and ADC value increases are smaller [12] as shown by the small ADC histogram shift between examinations 1 and 2 (Anastrozole and Goserelin therapy). When combination treatments are used, a synergistic, additive therapy effect can be observed clinically. This explains the greater ADC change in this case where Everolimus and Exemestane (mTOR inhibitor and hormonal therapy) were used together (examinations 3–6) resulting in two distinct peaks in the ADC histogram.

The phenomenon of ‘T2-shine through’ indicates a successful therapeutic effect with bone marrow edema. ‘T2-shine through’ can take a long time for high b-value signal intensity and ADC to decrease to normal levels [10]. The emergence of bone sclerosis, bone marrow fibrosis and/or return of bone marrow fat are part of repair processes, reducing high b-value signal intensity and lowering ADC values visible on the Ex9 images [10].

Contact

Dr. Danoob Dalili
Specialist Registrar Clinical Radiology
Imperial College Healthcare NHS Trust
St Mary's Hospital
Praed St
London W2 1NY
United Kingdom
Phone: +44 (0) 20 3312 6666
Dalili@doctors.org.uk



Prof. Anwar R. Padhani
Consultant Radiologist and
Professor of Cancer Imaging
Paul Strickland Scanner Centre
Mount Vernon Cancer Centre
Rickmansworth Road
Northwood, Middlesex HA6 2RN
United Kingdom
Phone (PA): +44-(0) 1923-844751
Fax: +44-(0) 1923-844600
anwar.padhani@stricklandscanner.org.uk



This latter phenomenon of decreasing ADC values with tissue repair highlights the need to evacuate all the acquired images (multiparametric assessments) for the correct interpretation of likely tissue disease status. So relying on ADC histograms alone may be misleading in the setting of tissue repair and recovery, making it necessary to take into account morphological appearances and quantitative parameters such as fat fraction and high b-value signal intensity to distinguish between healing processes from recurrent/residual cancer.

References

- Lin NU, Thomssen C, Cardoso F et al. European School of Oncology-Metastatic Breast Cancer Task Force. International guidelines for management of metastatic breast cancer (MBC) from the European School of Oncology (ESO)-MBC Task Force: Surveillance, staging, and evaluation of patients with early-stage and metastatic breast cancer. *Breast*. 2013; 22(3):203-10.
- Graham LJ, Shupe MP, Schneble EJ, et al. Current approaches and challenges in monitoring treatment responses in breast cancer. *J Cancer*. 2014 Jan 5;5(1):58-68.
- Harris L, Fritsche H, Mennel R, et al. American Society of Clinical Oncology. American Society of Clinical Oncology 2007 update of recommendations for the use of tumor markers in breast cancer. *J Clin Oncol*. 2007; 20;25(33):5287-312.
- Cardoso F, Costa A, Senkus E, et al. 3rd ESO-ESMO International Consensus Guidelines for Advanced Breast Cancer (ABC 3). *Ann Oncol*. 2017 Jan 1;28(1):16-33.
- Riedl CC, Pinker K, Ulaner GA, et al. Comparison of FDG-PET/CT and contrast-enhanced CT for monitoring therapy response in patients with metastatic breast cancer. *Eur J Nucl Med Mol Imaging*. 2017 [epub].
- Kosmin M, Makris A, Joshi PV, et al. The addition of whole-body magnetic resonance imaging to body computerised tomography alters treatment decisions in patients with metastatic breast cancer. *Eur J Cancer*. 2017; 77:109-116.
- Woolf DK, Padhani AR, Makris A. Assessing response to treatment of bone metastases from breast cancer: what should be the standard of care? *Ann Oncol*. 2015; 26(6):1048-57.
- Grimm R, Padhani AR. Whole-body Diffusion-weighted MR Image Analysis with syngo.via Frontier MR Total Tumor Load. *MAGNETOM Flash* 2017; 68(2), 73-75.
- Danoob Dalili, Anwar R. Padhani, Robert Grimm. Quantitative WB-MRI with ADC histogram analysis for demonstrating complex response of bone marrow metastatic disease. *MAGNETOM Flash* 2017; 69(3): 38–42.
- Padhani AR, Makris A, Gall P, et al. Therapy monitoring of skeletal metastases with whole-body diffusion MRI. *J Magn Reson Imaging*. 2014; 39(5):1049-78.
- Padhani AR, Lecouvet FE, Tunariu N, et al. METastasis Reporting and Data System for Prostate Cancer (MET-RADS): Practical Guidelines for Acquisition, Interpretation, and Reporting of Whole-body MRI-based Evaluations of Multiorgan Involvement in Advanced Prostate Cancer. *Eur Urol*. 2017; 71(1):81-92.
- Padhani, AR, Van Ree, K, Collins DJ, et al Assessing the Relation Between Bone Marrow Signal Intensity and Apparent Diffusion Coefficient in Diffusion-Weighted MRI. *American Journal of Roentgenology* 2013; 200(1), 163-170.
- Messiou C, Collins DJ, Morgan VA, Desouza NM. Optimising diffusion weighted MRI for imaging metastatic and myeloma bone disease and assessing reproducibility. *Eur Radiol*. 2011; 21(8):1713-8.
- Padhani AR. Observing endocrine therapy resistance in metastatic breast cancer with whole body MRI. *Magnetom FLASH* 2017; 68(2):80-83.